SAGA-HE-185-02 (hep-ph/0204242) May 28, 2002

Structure functions of the nucleon and nuclei in neutrino reactions

S. Kumano *

Department of Physics
Saga University
Saga, 840-8502, Japan

Invited talk given at the First International Workshop on
Neutrino-Nucleus Interactions in the Few GeV Region

KEK, Tsukuba, Japan, December 13 - 16, 2001

(talk on Dec. 13, 2001)

* Email: kumanos@cc.saga-u.ac.jp. URL: http://hs.phys.saga-u.ac.jp.

to be published in Nucl. Phys. B Supplement

Structure functions of the nucleon and nuclei in neutrino reactions

S. Kumano [a] *

[a]Department of Physics, Saga University, Saga, 840-8502, Japan

Determination of parton distribution functions in nuclei is important for calculating nuclear corrections in oscillation experiments, from which detailed information should be extracted on neutrino properties. First, nuclear parton distributions are discussed for explaining high-energy nuclear reaction data. Possible nuclear modification is explained for valence-quark and antiquark distributions. It is rather difficult to determine gluon distributions in nuclei. Next, reversing the topic, we discuss structure functions which could be investigated by neutrino reactions. Determination of polarized parton distributions in the nucleon is discussed in polarized neutrino reactions. In addition, neutrino reactions should be important for finding nuclear modification of valence-quark distributions at small x if structure function ratios F_3^A/F_3^D are measured for various nuclei.

1. Introduction

Corrections of nuclear effects become important for understanding neutrino cross sections, as their measurements become more accurate, in order to find the details of neutrino properties [1]. In this paper, the nuclear corrections are discussed in the high-energy region in terms of parton distribution functions (PDFs). Unpolarized PDFs in the nucleon have been investigated for many years, and they are well established from very small x to relatively large x. However, it is known that parton distributions in a nucleus are different from those in the nucleon. Such nuclear modification was first found by the European Muon Collaboration (EMC) at medium x.

Now, detailed nuclear modification is known in the structure function F_2 from small x to large x. In the first part of this paper, we discuss possible nuclear parton distributions which are extracted from deep-inelastic-scattering (DIS) experimental data [2] partly with Drell-Yan data [3]. The nuclear PDFs are defined at fixed Q^2 with a number of parameters, which are determined by a χ^2 analysis of the data. There are also other analyses in Ref. [4] by including the F_2^A/F_2^D and Drell-Yan data together with Q^2 dependent data of F_2^{Sn}/F_2^C. There are differences between these two groups, especially in the x dependent functional form of the initial PDFs. From the present data, it is rather difficult to determine nuclear gluon distributions; however, the Q^2 dependent data could impose some restrictions through Q^2 evolution equations [4]. We discuss an analysis method and results, from which useful computer subroutines are supplied [2] for calculating the nuclear PDFs numerically at given x and Q^2 points for a certain nucleus. The obtained nuclear PDFs could be used for application to high-energy nuclear reactions such as heavy-ion reactions [5] and neutrino-nucleus reactions [1], which are the topics under discussion at this workshop.

To the contrary, high-energy neutrino reactions should play an important role in determining the nuclear PDFs if accurate data are taken for structure function ratios to the one for the deuteron. However, it is not possible at this stage due to lack of accurate deuteron data. In future, there are possibilities to have neutrino factories, and we discuss possible PDF studies at such factories in the last part of this paper. In particular, we expect that the valence-quark distributions at small x could be investigated.

Future polarized neutrino measurements should be valuable for the studies of nucleon spin. It was revealed that quarks carry a small fraction of the nucleon spin in contradiction to a naive quark model prediction. The neutrino reactions have an advantage of measuring the spin

*kumanos@cc.saga-u.ac.jp, http://hs.phys.saga-u.ac.jp

content directly. In addition, polarized valence- and strange-quark distributions should be investigated.

The nuclear PDFs are explained in Sec. 2 for understanding nuclear corrections. Then, neutrino-nucleon and neutrino-nucleus reactions are discussed for better determination of PDFs in Sec. 3. Our studies are summarized in Sec. 4.

2. Parton distribution functions in nuclei

Nuclear medium effects have been investigated mainly in the structure function F_2. The ratio F_2^A/F_2^D is about 15% smaller than the one for a medium size nucleus at medium x, and it tends to increase at large x ($\sim$0.9). At small x, the ratio F_2^A/F_2^D decreases as x becomes smaller, which indicates nuclear shadowing phenomenon. A different physics mechanism, such as binding, Fermi motion, possible subnucleon effect, or multiple scattering, contributes to the modification in each x region [6]. Here, we do not address ourselves to such physical mechanisms, and we focus on nuclear parton distributions which are extracted from deep inelastic experimental data and Drell-Yan processes [2,3].

Nuclear modification of the PDFs is typically less than 20% for medium size nuclei. Because they are not much different from those in the nucleon, it is technically easier to investigate x dependent functional form of the nuclear modification rather than absolute nuclear PDFs. Furthermore, experimental nuclear structure functions are often shown by the ratio to the one for deuteron such as F_2^A/F_2^D. Therefore, we define a weight function $w_i(x, A, Z)$, which indicates the nuclear modification, by

$$f_i^A(x, Q_0^2) = w_i(x, A, Z)\, f_i(x, Q_0^2), \qquad (1)$$

where A and Z are the mass number and the atomic number, $f_i^A(x, Q_0^2)$ is the type-i parton distribution at Bjorken variable x and Q_0^2 in a nucleus, and $f_i(x, Q_0^2)$ is the corresponding distribution in the nucleon. Because a wide variety of date are not available in the nuclear case, flavor separation of antiquark distributions is not possible at this stage. Therefore, as the parton type i, we take f_i^A=u_v^A, d_v^A, $\bar{q}^A$, and g^A by assuming flavor symmetric antiquark distributions: $\bar{u}^A = \bar{d}^A = \bar{s}^A$ ($\equiv \bar{q}^A$). As one of the widely used distributions in the nucleon, the leading-order (LO) distributions of the MRST parametrization [7] are used in our numerical analysis.

The weight functions are parametrized and they are determined by high-energy nuclear reaction data. The nuclear modification part is assumed to have the following functional form:

$$w_i(x, A, Z) = 1 + \left(1 - \frac{1}{A^{1/3}}\right) \times \frac{a_i(A, Z) + b_i x + c_i x^2 + d_i x^3}{(1-x)^{\beta_i}}, \qquad (2)$$

where a_i, b_i, c_i, d_i, and β_i are parameters, which are determined by a χ^2 analysis. In the first analysis [2], the $1/A^{1/3}$ dependence is assumed for simplicity by considering volume and surface type contributions to the cross section. We will determine this factor from the experimental data in future analyses.

The nuclear PDFs are defined at fixed Q^2 ($\equiv Q_0^2$), whereas the data are taken at various Q^2 points. The initial point is selected as $Q_0^2 = 1$ GeV^2. In order to make a χ^2 analysis with the data, the parton distributions are evolved to the experimental Q^2 points by the ordinary DGLAP evolution equations [8]. The LO analysis is made, so that the expression of F_2^A is give by

$$F_2^A(x, Q^2) = \sum_q e_q^2\, x\, [q^A(x, Q^2) + \bar{q}^A(x, Q^2)], \qquad (3)$$

where q^A and $\bar{q}^A$ are the quark and antiquark distributions in the nucleus A, and e_q is the quark charge. The total χ^2 is given by

$$\chi^2 = \sum_j \frac{(R_j^{data} - R_j^{theo})^2}{(\sigma_j^{data})^2}. \qquad (4)$$

The notation R is defined by the structure-function ratio $R = F_2^A/F_2^D$ [2], where D denotes the deuteron. In Ref. [3], Drell-Yan cross-section ratios are added to the above χ^2 definition.

There are still many parameters to be determined by the data. The nuclear distributions should be constrained by the three conditions:

charge, baryon-number, and momentum conservations. They are expressed by the parton distributions as

$$\begin{aligned} \text{Charge: } Z &= \int dx\, \frac{A}{3}\left(2\, u_v^A - d_v^A\right), \\ \text{Baryon \#: } A &= \int dx\, \frac{A}{3}\left(u_v^A + d_v^A\right), \\ \text{Momentum: } A &= \int dx\, A\, x\left(u_v^A + d_v^A + 6\,\bar{q}^A + g^A\right), \end{aligned} \tag{5}$$

where the parton distributions are given by those per nucleon as obvious from Eqs. (1) and (2). Therefore, three parameters can be fixed by these conditions. Other parameters are determined so as to minimize the total χ^2 in Eq. (4).

The analysis with the weight functions in Eq. (2) is called a cubic polynomial type. Another analysis was also done without the $d_i x^3$ term, and it is called a quadratic polynomial type. Because quadratic results are similar to the cubic ones [2], they are not shown in the following discussions. As a result of the cubic type analysis, the χ^2_{min} per degrees of freedom becomes $\chi^2_{min}/d.o.f.$=1.82 for the 309 total data points. Obtained distributions are compared with some of the used data in Figs. 1, 2, and 3. In these figures, the solid curves are the fit results in the cubic analysis at Q^2=5 GeV^2. Because the data are taken in general at different Q^2 points, the curves cannot be directly compared with the data. However, considering that the Q^2 dependence of the ratio R is not fairly large, we find that the curves agree with the experimental data from small x to large x.

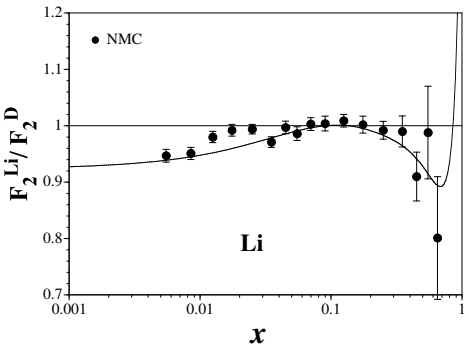

Figure 1. Comparison with the lithium data. The curve indicates the cubic analysis result at Q^2=5 GeV^2.

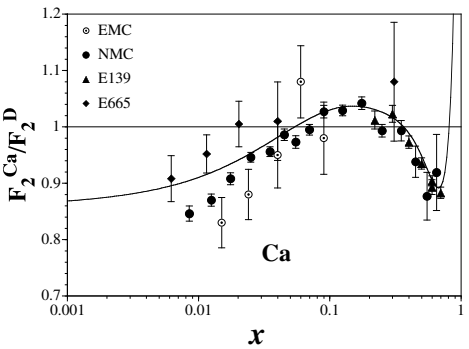

Figure 2. Comparison with the calcium data.

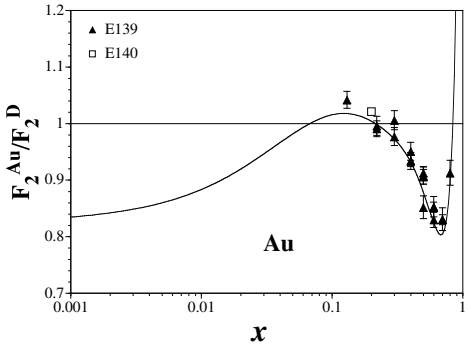

Figure 3. Comparison with the gold data.

From the analyses, we obtain the weight functions for the calcium nucleus in Fig. 4. By definition, the curves indicate the nuclear modification at Q^2=1 GeV^2. The valence-quark distributions show the depletion at $x \sim 0.6$ so as to explain the EMC effect of F_2 at medium x, and they increase at large x to explain the Fermi-motion part of the F_2 data. Because the valence distributions do not contribute to F_2 at small x, their determination is difficult. As discussed in the next section, if accurate neutrino data could be taken for the ratio F_3^A/F_3^D in future, the determination becomes possible. The nuclear gluon distributions are difficult to be determined in the whole x region at least at this stage. Because the antiquark distributions dominate the structure function F_2^A

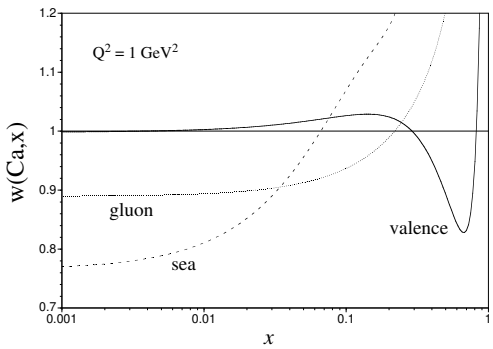

Figure 4. Obtained weight functions are shown for the valence-quark, antiquark, and gluon distributions in the calcium nucleus.

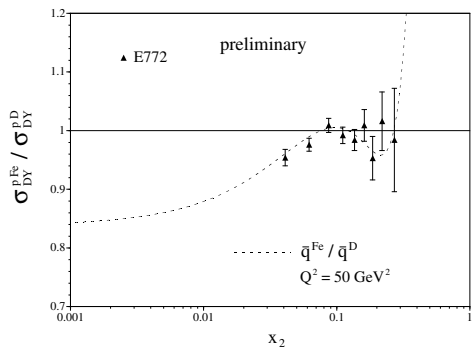

Figure 5. Experimental Drell-Yan cross section ratios are compared with the calculated antiquark ratio $\bar{q}^{Fe}/\bar{q}^{D}$.

at small x, their determination is possible in the small x region. However, they cannot be fixed in the medium and large x regions.

Drell-Yan data are valuable for determining the antiquark distributions, and their analysis is in progress [3]. The Drell-Yan measurements are shown by the ratios $\sigma_{DY}^{pA}/\sigma_{DY}^{pD}$ and $\sigma_{DY}^{pA}/\sigma_{DY}^{pA'(\neq D)}$. Parton momentum fractions are expressed x_1 and x_2 in the proton and a nucleus, respectively. In the large x_F ($=x_1 - x_2$) region, namely in the small x_2 region, the Drell-Yan cross-section ratio $\sigma_{DY}^{pA}/\sigma_{DY}^{pD}$ is roughly proportional to the antiquark-distribution ratio $\bar{q}^{A}/\bar{q}^{D}$. A typical result is shown in Fig. 5 together with the experimental data. The dashed curve is the antiquark ratio $\bar{q}^{Fe}/\bar{q}^{D}$ at Q^2=50 GeV^2. It is almost equal to the cross section ratio $\sigma_{DY}^{pFe}/\sigma_{DY}^{pD}$ except for the large x_2 region ($x_2 > 0.2$). The theoretical curve is based on our preliminary analysis results.

As shown in the figure, the antiquark distributions are restricted in the region $x \sim 0.1$, where there is almost no nuclear modification. Therefore, the Drell-Yan data are valuable for finding the antiquark distributions in the medium x region [4]. We hope to report the analysis results with the Drell-Yan data in the near future [3].

From the χ^2 analysis results of Ref. [2], we provide subroutines for calculating the parton distributions at any x and Q^2 for a given nucleus. The codes could be obtained from our web site [2]. Alternatively, one could use the obtained analytical expressions of the weight functions $w_i(x, A, Z)$ for calculating the parton distributions.

There are other analyses by Eskola, Honkanen, Kolhinen, Ruuskanen, and Salgado [4], and their results are rather different from the ones discussed in this section. First, for the initial distributions, namely the weight functions in Eq. (2), they divided the x region into three parts: shadowing, EMC, and Fermi-motion regions. Then, a different x dependent functional form is employed in each x region for fitting the DIS experimental results with the Drell-Yan data. However, as far as we are aware, the details of the analysis, especially χ^2 values, have not been reported yet. In our first version [2], the Drell-Yan data were not included in the analysis partly because we intended to find how well the PDFs could be determined solely by the F_2^A/F_2^D data. Therefore, the antiquark modification increased monotonically as x becomes larger in contrast with the one in Ref. [4], where the modification is suppressed in the $x \sim 0.1$ region. In the same way, the gluon distributions at medium x are also different; however, they could not be determined well in any case in the present situation. Obviously, these analyses are still premature, so that nuclear parametrizations should be investigated further by technical refinements with new experimental data.

3. Structure functions in neutrino reactions

In the previous section, we discussed the determination of the nuclear PDFs by using the electron and muon DIS data partly with the Drell-Yan data. In this section, we discuss the role of high-energy neutrino scattering in the determination of the PDFs in the nucleon and nuclei.

3.1. Polarized parton distributions

Neutrino reaction data have been used for extracting the unpolarized PDFs in the nucleon although actual targets are mainly the iron. They are valuable especially for determining the strange- and valence-quark distributions. Now, the major part of the unpolarized PDFs is well known, and our interest tends toward polarized PDFs in the nucleon. Available experimental information is limited for the polarized PDFs in the sense that the data come mainly from inclusive electron and muon DIS and some semi-inclusive processes. Furthermore, the small x ($x \sim 10^{-4}$) part is not measured yet, which makes it difficult to determine polarized antiquark distributions. This fact affects the determination of the quark spin content $\Delta\Sigma$, which has been controversial for a decade. Future polarized neutrino reaction data should be able to provide important information on the polarized distributions and the quark spin content.

In polarized neutrino-proton reactions, structure functions $g_1^{\nu p}$ and $g_1^{\bar{\nu} p}$ are expressed by the parton distributions [9]:

$$\begin{aligned} g_1^{\nu p} =& \Delta d + \Delta s + \Delta \bar{u} + \Delta \bar{c}, \\ g_1^{\bar{\nu} p} =& \Delta u + \Delta c + \Delta \bar{d} + \Delta \bar{s}, \end{aligned} \tag{6}$$

in the leading order (LO). Combining these expressions, we find

$$\int dx \, (g_1^{\nu p} + g_1^{\bar{\nu} p}) = \Delta\Sigma. \tag{7}$$

Although there are higher-order corrections, the integral is directly proportional to the quark spin content $\Delta\Sigma$ of the nucleon in the LO. This is an advantage of the neutrino reactions in comparison with the electron and muon scattering, where $\Delta\Sigma$ cannot be observed directly due to the quark charge factor e_q^2. In fact, the obtained spin content from the present DIS data ranges from $\Delta\Sigma$=0.05 to 0.3. This uncertainty comes from the difficulty in determining the polarized antiquark distributions at small x [10].

In addition to this advantage, the neutrino reactions provide valuable information by the parity-violating structure functions g_3, g_4, and g_5 [9,11]. In the parton model, they are expressed as [9]

$$\begin{aligned} (g_4^{\nu p} + g_5^{\nu p})/2x &= g_3^{\nu p} \\ &= -(\Delta d + \Delta s - \Delta \bar{u} - \Delta \bar{c}), \\ (g_4^{\bar{\nu} p} + g_5^{\bar{\nu} p})/2x &= g_3^{\bar{\nu} p} \\ &= -(\Delta u + \Delta c - \Delta \bar{d} - \Delta \bar{s}). \end{aligned} \tag{8}$$

Combining these structure functions, we have

$$\begin{aligned} g_3^{\nu p} + g_3^{\bar{\nu} p} &= -(\Delta u_v + \Delta d_v) - (\Delta s - \Delta \bar{s}) \\ &\quad -(\Delta c - \Delta \bar{c}), \\ \frac{1}{2}\,[\, g_3^{\bar{\nu}(p+n)} - g_3^{\nu(p+n)} \,] &= (\Delta s + \Delta \bar{s}) - (\Delta c + \Delta \bar{c}). \end{aligned} \tag{9}$$

Because the differences $\Delta s - \Delta \bar{s}$ and $\Delta c - \Delta \bar{c}$ are expected to be small, the combination $g_3^{\nu p} + g_3^{\bar{\nu} p}$ could be used for finding the polarized valence-quark distributions. On the other hand, the proton and neutron combination $g_3^{\bar{\nu}(p+n)} - g_3^{\nu(p+n)}$ is valuable for determining the strange and charm quark distributions. Furthermore, the strange-quark polarization Δs could be investigated by the opposite-sign dimuon events. In this way, the neutrino scattering should be able to provide valuable information on the polarized parton distributions, which cannot be probed by the electron scattering and hadron-hadron reactions.

3.2. Parton distributions in nuclei

We have discussed the nuclear parton distributions in Sec. 2. We found that their determination is not straightforward by the electron and muon scattering data even together Drell-Yan cross sections. Neutrino-nucleus reactions should be able to provide valuable information. Actually, there are many available neutrino-iron scattering data.

However, because there is no accurate neutrino-deuteron DIS data, it is almost impossible to investigate the nuclear modification at this stage. If an intense neutrino beam becomes available at a neutrino factory [12], it becomes possible to investigate neutrino reactions with the proton, deuteron, and various nuclei.

It is especially interesting to investigate the structure function F_3, which does not exist in the electron and muon scattering. A combination of neutrino and anti-neutrino cross-sections is expressed in the parton model as

$$\frac{1}{4}\,[\,F_3^{\nu(p+n)} + F_3^{\bar{\nu}(p+n)}\,] = u_v + d_v + (s-\bar{s}) + (c-\bar{c})\ . \qquad (10)$$

The differences between the antiquark distributions are considered to be small, so that the structure function F_3 is appropriate for probing the nuclear modification of the valence-quark distributions. Because the ratio F_3^A/F_3^D should be equal to F_2^A/F_2^D in the LO at medium and large x, the advantage of the neutrino reactions is to investigate the valence-quark modification at small x. For example, the analysis results in Sec. 2 indicate very small shadowing at small x as shown by the solid curve in Fig. 6. On the other hand, some shadowing models [13] produce the modification which is similar to the one for the structure function F_2, and it is shown by the dotted curve. It indicates strong shadowing in the valence-quark distributions. Because the EMC effect of F_2 at medium x should be explained by the valence-quark modification, both curves have depletion at $x \sim 0.5$. Due to the baryon number conservation in Eq. (5), the modification should be positive in the region, $x \sim 0.1$. However, the valence-quark distributions are small in the small x region, so that they are not strongly constrained by the baryon number. At this stage, it is not even obvious whether they show shadowing behavior or antishadowing at small x. It is very important to determine the nuclear valence-quark distributions at small x in order to find accurate antiquark and gluon distributions in nuclei and to test nuclear shadowing models. However, there is no information on the valence-quark shadowing at this stage because the antiquark distributions dominate the structure function F_2 at small x.

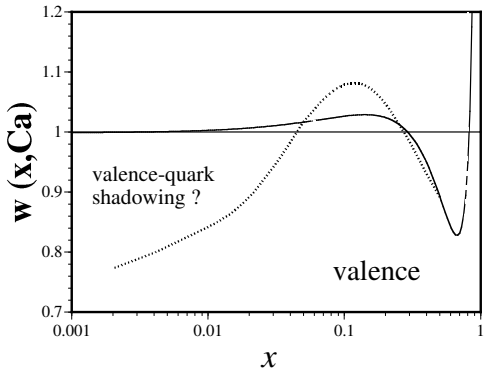

Figure 6. Nuclear modification of the valence-quark distributions.

In addition, if accurate experimental data are taken on neutrino-nucleus reactions, it becomes possible to investigate nuclear antiquark distributions by combing different structure functions in the similar way to the polarized case of Eq. (9). A future neutrino factory should play an important role for the determination of the nuclear parton distributions. Furthermore, the details of antiquark flavor asymmetry and isospin violation could be investigated in the nucleon and nuclei by combining different structure functions in the neutrino reactions [14].

4. Summary

Nuclear parton distribution functions are determined by high-energy nuclear reaction data, so that they could be used for calculating nuclear corrections in high-energy neutrino reactions. Nuclear shadowing at small x, the EMC effect at medium x, and Fermi motion at large x are well explained by the parametrization. However, precise determination is still difficult in some x regions. For example, it is not straightforward to obtain the valence-quark distributions at small x and the antiquark distributions at medium x. The gluon distributions could not be fixed well in the whole x region. The nuclear PDF studies are still at the preliminary stage; therefore, future

theoretical and experimental efforts are crucial for the precise determination.

On the other hand, if a neutrino factory is built in future, the details of the parton distributions in the nucleon and nuclei could be investigated. We showed that the valence-quark shadowing should be clarified by the measurements of structure functions F_3 for various nuclei. Furthermore, polarized neutrino reactions should clarify the issue of quark spin content in the nucleon by the measurements of the spin dependent structure functions. The polarized measurements should lead to better determination of the polarized PDFs.

Acknowledgments

S.K. was supported by the Grant-in-Aid for Scientific Research from the Japanese Ministry of Education, Culture, Sports, Science, and Technology. He thanks M. Sakuda for his invitation and financial support for participating in this workshop.

REFERENCES

1. E. A. Paschos and J. Y. Yu, Phys. Rev. D65 (2002) 033002; E. A. Paschos, talk at this workshop.
2. M. Hirai, S. Kumano, and M. Miyama, Phys. Rev. D64 (2001) 034003. See http://hs.phys.saga-u.ac.jp/nuclp.html.
3. M. Hirai and S. Kumano, research in progress.
4. K. J. Eskola, V. J. Kolhinen, and P. V. Ruuskanen, Nucl. Phys. B535 (1998) 351; K. J. Eskola, H. Honkanen, V. J. Kolhinen, P. V. Ruuskanen, and C. A. Salgado, hep-ph/0110348.
5. Shi-yuan Li and Xin-Nian Wang, Phys. Lett. B527 (2002) 85; X. Zhang and G. Fai, hep-ph/0202029.
6. For a summary, see D. F. Geesaman, K. Saito, and A. W. Thomas, Ann. Rev. Nucl. Part. Sci. 45 (1995) 337.
7. A. D. Martin, R. G. Roberts, W. J. Stirling, and R. S. Thorne, Eur. Phys. J. C4 (1998) 463.
8. M. Miyama and S. Kumano, Comput. Phys. Commun. 94 (1996) 185. See http://hs.phys.saga-u.ac.jp/program.html.
9. B. Lampe and E. Reya, Phys. Rep. 332 (2000) 1.
10. Asymmetry Analysis Collaboration (AAC), Y. Goto *et. al.*, Phys. Rev. D62 (2000) 034017.
11. J. Blümlein, pp.126-129 in High Energy Spin Physics, Riken Review No. 28 (2000), edited by S. Kumano *et. al.*.
12. C. Albright *et. al.*, hep-ex/0008064; M. L. Mangano *et. al.*, hep-ph/0105155; J. G. Morfin, talk at this workshop.
13. L. L. Frankfurt, M. I. Strikman, and S. Liuti, Phys. Rev. Lett. 65 (1990) 1725; R. Kobayashi, S. Kumano, and M. Miyama, Phys. Lett. B354 (1995) 465; S. A. Kulagin, Nucl. Phys. A640 (1998) 435.
14. S. Kumano, Phys. Rep. 303 (1998) 183.